FERMILAB-CONF-75-108-E
CALT 68-494
ENERGY RESEARCH AND
DEVELOPMENT REPORT

CALIBRATION OF A SAMPLING TOTAL ABSORPTION DETECTOR DESIGNED FOR NEUTRINO EXPERIMENTS *

B. C. Barish, J. F. Bartlett, A. Bodek, K. W. Brown, D. Buchholz, F. Jacquet†, F. S. Merritt, F. J. Sciulli, L. Stutte, H. Suter††

California Institute of Technology, Pasadena, California 91125, U.S.A.

and

H. E. Fisk and G. Krafczyk

Fermilab, Batavia, Illinois 60510, U.S.A.

May 1975

(Revised July 1975)

Abstract

A sampling total absorption detector was calibrated at Fermilab for energies in the range 5 to 250 GeV. The calorimeter consisted of a sandwich of scintillator slabs and 4" thick steel plates. Energy resolutions (rms) of ± 33%, ± 16%, and ±9% were achieved for the energies 10, 50, and 150 GeV respectively.

---

* Work supported in part by the U.S. Energy Research and Development Administration. Prepared under Contract AT(11-1)-68 for the San Francisco Operations Office.

† On leave of absence from Ecole' Polytechnique, Paris, France.

†† Swiss National Fund for Scientific Research Fellow.

Recent neutrino experiments[1] performed in the Fermilab narrow band neutrino beam have used a large area sampling total absorption[2] detector. The total absorption detector serves the dual purpose of being a target as well as a hadron calorimeter. This massive detector contains 143 tons of steel in the form of seventy steel slabs, each 5' x 5' in area and 4" thick. The energy of the final state hadrons released in neutrino interactions such as

$$\nu + \text{Nucleus} \rightarrow \mu^- + \text{hadrons} \qquad (1)$$

and

$$\nu + \text{Nucleus} \rightarrow \nu + \text{hadrons} \qquad (2)$$

is measured by seventy scintillation counters placed after every 4" of steel (one collision length). The final state hadrons initiate a shower which is sampled by the scintillation counters. The sampling every nuclear collision length in steel is sufficient to allow the measurement of the energy of a 50 GeV shower to an rms accuracy of ± 16%.

Because of the large mass of the target calorimeter, it is impractical to move it into a hadron beam for the purpose of calibration.[3] Instead, a scale model calorimeter of similar design but reduced transverse and longitudinal dimensions was constructed and placed in hadron beams of well defined energies at Fermilab. This scaled down model was described in an earlier publication[4], where results of an early calibration run at 200 GeV were reported. In this publication we report results from the more recent calibration runs for beam energies between 5 and 250 GeV. The most extensive measurements were done in August of 1974. Less extensive measurements were done during June and July of 1974.

A schematic of the scaled-down calorimeter is shown in Fig. 1. It consists of 14 modules, each made of a 4" thick plate of steel (10" x 14" in area) followed by a 3/8" thick plastic scintillator. The 14 scintillation counters were placed in the 1.1" thick air gaps between the steel plates. This scaled-down calorimeter is long enough to contain longitudinally the shower initiated by the incident hadrons at present Fermilab energies. In front of the calorimeter three counters T1, T2, and T3 are used to signal a single charged particle incident on the detector. The trigger is T1 T2 $\overline{T3}$. To provide a calibrating one particle signal, the steel plates in the calorimeter are removable, in which case the particles pass through the counters without interacting. Each scintillator is equipped with its own phototube (RCA6655); the signals are separately pulse height analyzed for each event, (using LRS 227 quad integrators) and all data are written on magnetic tape.

The calorimeter was placed in the hadron beam[6] that is normally used for the 30" bubble chamber in the neutrino area at Fermilab. The primary 300 GeV proton beam was directed on to a production target. A momentum and sign selected secondary beam was transported to the location of the calorimeter 1650 feet downstream by a series of bending and focusing magnets. The beam was primarily composed of hadrons (mostly protons and pions for positive sign selection and mostly pions for negative sign selection) with a small muon component. At energies less than 100 GeV there the beam contained a substantial electron contamination (30% at 50 GeV). The electron component was removed prior to the final momentum selection by a 1" thick lead absorber placed 590 feet upstream of the calorimeter.

Data were first taken with all the steel removed in order to calibrate the 14 counters with singly ionizing hadrons. The signals from the photomultipliers were amplified by a factor of 35 for this calibration. The pulse height distribution for singly ionizing 150 GeV hadrons in the first counter is shown in figure 2a. Runs were taken with positive sign selected beams at 10 and 150 GeV, and with negative sign selected beams at 20 and 100 GeV. The peak positions (i.e. the most probable value or the mode of the distribution) were independent of the energy or sign of the hadron beam. The average peak positions in the 14 counters were the same at 10, 20, 100 and 150 GeV to $\pm$ 0.4%. With the steel back in place, we repeated the test with positive sign selected muons at 30 and 50 GeV. The pulse height distribution of singly ionizing muons in the first counter is shown in figure 2b. Here also the peak positions of singly ionizing muons were independent of energy and equal to the peak for singly ionizing hadrons to $\pm$ 0.4%. The curves that are shown correspond to those from a simple model in which each ionizing particle produces a pulse height which is Poisson distributed and in addition can produce a delta ray, traversing the 3/8" of scintillator, with a probability of 0.12.

We use the most probable value to define a single ionizing pulse because theoretical calculations[5] indicate that, unlike the mean value, the most probable value is independent of energy for energies greater than 5 GeV. This fact is corroborated by the above described studies. The pulse height distribution for non-interacting straight through muons summed over the 14 counters is shown in figure 3, where the abscissa is the number of equivalent singly ionizing particles. The steel plates were back in place for this test. A Gaussian fit to the distribution yields a mean of 17.9 equivalent particles and a standard deviation of 2.4. The difference between 14.0 and 17.9 is also a reflection of

the difference between the mean energy deposition and the most probable energy deposition in a counter by 50 GeV muons.

The peak positions for singly ionizing straight through muons are also used to calibrate the counters of the large area calorimeter. The hadron shower pulse heights in both the large area calorimeter and in the scaled-down model are expressed in terms of the equivalent number of singly ionizing particles. When expressed that way, the calibration and resolution of the scale model should be the same as that of the large area calorimeter.

With the steel plates back in place we recorded hadron shower events for a variety of incident energies ranging from 5 to 250 GeV. The signals were not amplified in this case, because hadron showers give much larger pulse height than those of singly ionizing particles. The pulse height distributions summed over the 14 counters for hadron energies of 5, 10, 20, 30, 50, 100, 150 and 250 GeV are shown in figures 4a and 4b, where the abscissa is the number of equivalent singly ionizing particles in the shower. The distributions that are shown represent only hadron events which satisfied conditions designed to discriminate against background events such as non-interacting muons and low energy electrons (e.g. electrons from interactions in the beam pipe, decays, etc.). Also, criteria that ensured the containment of the hadron shower within the scaled-down calorimeter were applied. These conditions are discussed below.

Background low energy electrons were characterized by a large pulse in the first counter, a smaller pulse in the second counter and no signal in the third counter. These background electrons were not a serious problem at energies greater than 30 GeV, as at those energies the hadron shower events were more numerous than background events, and the pulse heights summed over the 14 counters were much larger for hadron events than for background events. At energies less than 30 GeV, the electron background was removed by requiring the pulse height in the third counter to be larger than a minimum value. The muon background which yielded a peak at 17.9 equivalent particles was only important at 5 and 10 GeV where the hadron showers were small. At those energies muons were recognized by the presence of a penetrating particle in the back counters of the calorimeter. Additional discrimination against muons was obtained by forcing an interaction in the first module. At high energies, the requirement of an interaction in the first module (obtained by requiring the pulse height in the first counter to be larger than a minimum value) ensured the longitudinal containment of the shower and enabled us to study the shower development from the point of the primary interaction. This more nearly simulates the case of a neutrino interaction in the

large calorimeter where we know the vertex position. In order to avoid a bias in favor of large hadron showers (i.e. showers with a large electromagnetic component) we never required the number of particles in any counter to be more than 10% of the average number of particles in that counter for typical hadron showers. A summary of the event selection conditions is given in Appendix A. Also given in the Appendix are the shower development tables which contain the mean number of particles in each counter for all the incident energies that were studied as well as the mean fraction of the energy that is deposited in each counter. The shower development tables indicate that the longitudinal containment of the shower is complete for energies up to 150 GeV (when an interaction is forced in the first counter). At the higher energies, a 1% or 2% energy loss out the back of the calorimeter cannot be ruled out.

We also investigated the transverse containment of the shower by aiming the incident beam at various distances from the edge of the calorimeter. This type of data provide only an indirect[7] measure of the transverse containment of the shower. Such a study done at 150 GeV indicated that there is a small energy leakage out the side of about 2.2%. The side leakage at 200 and 250 GeV was not investigated but is expected to be similar.[8] The large area (5'x5') calorimeter used in the neutrino experiment is large enough to transversely contain the hadron shower; therefore, the means of the distributions at 150, 200 and 250 GeV were corrected by a multiplicative factor of 1.022. Similar studies done at the lower energies were less extensive and were inconclusive.[7] No side loss corrections were applied to the lower energy data. Monte Carlo calculations[8] indicate that the side loss may be on the order of 1% to 3% for $E > 50$ GeV, and may be as large as 6% at $E = 5$ GeV.

The distributions of total pulse height (summed over all 14 counters) of hadron showers in the calorimeter were found to be best represented by Poisson distributions (see Appendix C), especially at low energies. The best fit Poisson distributions are drawn on top of the data in figures 4a and 4b. Gaussian distributions (with the negative tails truncated) which have the same means and standard deviations as those of the Poisson distributions provide fair fits to the data. The Poisson fit means and standard deviations are given in Table I. The errors that are given are point to point errors (the errors in the means for the 200 and 250 GeV data are larger because they include an additional 5% normalization error due to equipment related difficulties encountered during the June run).

TABLE I.

Hadron shower energy deposition in the calorimeter expressed in terms of equivalent number of singly ionizing particles.

Run	Sign Selection	Momentum (GeV)	Mean	σ/Mean
August	-	5	18.2 ± 4	0.384 ± 0.200
August	-	10	52.7 ± 5	0.331 ± 0.031
August	-	20	106.3 ± 4	0.253 ± 0.010
August	-	30	164.5 ± 7	0.199 ± 0.010
August	-	50	269.0 ± 5	0.158 ± 0.007
August	-	100	538.0 ± 5	0.111 ± 0.007
July	+	150	808.0 ± 5	0.089 ± 0.004
June	-	200	1056.0 ± 53	0.079 ± 0.004
June	-	250	1287.0 ± 65	0.073 ± 0.004

The overall systematic error in the means is estimated at ±5%. The uncertainty in the energy loss out the sides leads to an additional error in the corrected means varying from 2% at the highest energy to 6% at the lowest energy. The Monte-Carlo[8] calculations indicate that the resolution of a calorimeter where no energy is lost out the sides may be narrower than what we measured by amounts varying from 5% at the highest energy to 20% at the lowest energy. These uncertainties will be greatly reduced with further investigations of the lateral containment of the shower.

The low energy data ($E \leq 30$ GeV), given in Table I, include a small correction to account for the fact that the primary interaction in neutrino reactions can occur uniformly throughout the 4" of steel while the primary interaction of the hadron beam tends to occur in the first part of the steel. This correction is described in Appendix B.

An interesting quantity to calculate is the fractional observed energy, i.e. the energy that is not lost in nuclear disintegrations. This quantity can be obtained approximately by a comparison of muon and hadron pulse heights. The

assumption involved is that the mean energy deposition of charged particles in the scintillator is proportional to the mean energy loss due to ionization in the steel. Under the above assumption, the difference between muon and hadron pulse heights is due to the unobserved energy loss in nuclear disintegrations initiated by the hadrons. The mean pulse height of 50 GeV muons traversing the 14 modules of the calorimeters is 17.9 ± 2.0 singly ionizing signals. Using the mean DE/DX value of 16.09 MeV/cm for 50 GeV muons in steel,[9] we find that a 50 GeV muon loses 2.287 GeV while traversing the calorimeter. Therefore, our definition of a singly ionizing signal corresponds to 2.287/17.9 GeV or 127.8 MeV. The mean pulse height of a 50 GeV hadron shower is 269 ± 5 singly ionizing signals or 34.4 GeV. This means that the fractional observed energy for hadrons in our calorimeter is 69% at 50 GeV. Another method of obtaining a measure of the fractional observed energy is by the direct comparison of electron and hadron pulse heights. This method (see Appendix B) yields the value of 80% for the fractional observed energy at 50 GeV.

The dependence of the peak position on energy was very close to linear for hadron showers completely contained in the calorimeter. The following fit provides a good representation of the data (see figure 5a)

$$\text{mean} = \frac{5.428\ T^2}{T + 0.721} \tag{3}$$

where the mean is expressed in number of equivalent singly ionizing particles, and T is the kinetic energy[10] of the incident hadron in GeV. The choice of the above functional form (eq.3) for the parametrization of the mean as a function of energy was motivated by the fact that Monte-Carlo[8] calculations indicate that the fractional observed energy should be smaller at lower energies.[11]

A good representation of the dependence of the rms resolution (σ/mean) on energy is provided by the fit (see figure 5b)

$$\text{Resolution (rms)} = 1.105 / \sqrt{T} \tag{4}$$

where the kinetic energy[10] T is in GeV. The data and the fit are shown in figure 5b.

By making appropriate sums of the calorimeter counters, we can investigate the effects of different counter spacing on resolution (for spacing greater than the nominal 4"). For example, adding the even counters allows a measurement of the resolution with 8" spacing (i.e. 8" of steel between scintillators). Such a study was done in the early calibration run[4] at 200 GeV. The results of that study are shown in figure 6 where the resolution is plotted vs. amount of steel between any two counters. The dependence is linear between 4" and 12" (the curves are drawn to guide the eye). The pulse height distributions summed over the 7 even counters (8" spacing) are shown in figures 7a and 7b. Table II shows a comparison between

the resolution with 4" spacing and the resolution with 8" spacing for energies investigated in the present study. The resolution with 8" spacing is roughly twice the resolution with 4" spacing. It is not expected that this linear relation continues for spacing smaller than 4" (as shown by othe published data[8]).

The above result is important because neutrino interactions in the large area calorimeter initiate hadron final state showers with mean momenta in a direction not necessarily normal to the plates of the calorimeter. A hadron shower produced at an angle θ_H with respect to the axis of the calorimeter will have a calibration which is independent of θ_H. This is because although the effective steel spacing is increased by a factor of $1/\cos\theta_H$, the amount of light produced by each secondary particle is increased by the same factor as the particles are traversing the scintillator at an angle. The resolution on the other hand will be that of a calorimeter of steel spacing equal to $4"/\cos\theta_H$. The results presented in Table II indicate that for small angles the resolution is directly proportional to $1/\cos\theta_H$.

TABLE II.

Comparison of the resolutions of calorimeters with 4" and 8" steel spacing.

Momentum(GeV)	Resolution 4" steel	Resolution 8" steel	Ratio 8"/4"
10	0.331	0.710	2.15
20	0.253	0.444	1.76
30	0.199	0.367	1.84
50	0.158	0.319	2.02
100	0.111	0.225	2.03
150	0.089	0.167	1.88
200	0.079	0.160	2.03
250	0.072	0.148	2.07

Further studies of calorimeters of various steel spacing are planned. Special emphasis will be placed on studies of the transverse containment of hadron showers and on the behavior at low ($E < 20$ GeV) beam energies. Also planned are studies of the low and high energy tails of the distributions and the development of an algorithm to improve the resolution by using the information in the longitudinal development of the shower.

We wish to acknowledge the help of the Fermilab/Neutrino Area staff.

Appendix A: Shower Development Tables

The mean number of particles in each counter for various incident momenta are given in Table A.1. The symbol + denotes positively charged hadrons and the symbol - denotes negatively charged hadrons. Because of equipment related difficulties encountered during the June run, there are larger uncertainties in the counter to counter calibrations of the 200 and 250 GeV data. The overall normalization of that data is correct to ±5% because the mean for the sum of 14 counters measured with 150 GeV hadrons in the June run agreed with later measurements taken with 150 GeV hadrons during the July run.

TABLE A.1

Mean number of particles in each counter for various incident energies.

Counter	-5 GeV	-10 GeV	-20 GeV	-30 GeV	-50 GeV	-100 GeV	+150 GeV	-200 GeV	-250 GeV
1	11.4	21.1	36.2	51.4	66.0	108.0	138.0	193.0	207.8
2	5.1	14.1	32.2	50.6	83.5	157.0	198.0	247.1	283.3
3	1.4	6.2	15.3	22.2	41.9	87.7	140.0	183.8	227.6
4	0.1	4.4	9.1	14.0	27.7	59.3	91.8	107.2	132.4
5	0.0	2.0	5.0	9.4	18.9	43.1	73.1	102.1	129.9
6	0.0	1.5	3.0	5.4	11.3	27.1	48.3	57.2	74.2
7	0.0	0.8	1.7	3.8	7.4	19.5	35.9	43.9	60.6
8	0.0	0.4	0.8	2.1	4.4	12.1	23.8	30.6	40.8
9	0.0	0.3	0.5	1.0	3.0	8.4	17.1	20.4	29.7
10	0.0	0.2	0.3	0.7	1.8	5.4	13.0	16.3	23.5
11	0.0	0.1	0.1	0.5	1.4	3.7	7.4	8.2	12.4
12	0.0	0.1	0.1	0.2	0.7	2.2	4.3	5.1	7.4
13	0.0	0.1	0.1	0.1	0.4	1.5	2.7	3.1	4.9
14	0.0	0.1	0.1	0.2	0.5	1.2	2.6	2.0	3.7

The shower development can also be described in terms of the average fractional energy deposition in each counter, i.e. $< N_i/N_{total} >$, where N_i is the number of particles in counter number i, and $N_{total} = \sum_i N_i$.

TABLE A.2

The mean fractional energy deposition in each counter for various incident momenta.

Counter	-5 GeV	-10 GeV	-20 GeV	-30 GeV	-50 GeV	-100 GeV	+150 GeV	-200 GeV	-250 GeV
1	0.680	0.413	0.346	0.319	0.246	0.200	0.174	0.189	0.168
2	0.224	0.276	0.306	0.310	0.306	0.288	0.249	0.242	0.229
3	0.079	0.123	0.146	0.139	0.156	0.163	0.175	0.180	0.184
4	0.017	0.083	0.087	0.088	0.105	0.112	0.116	0.105	0.107
5	0.000	0.038	0.048	0.057	0.070	0.081	0.092	0.100	0.105
6	0.000	0.027	0.027	0.034	0.053	0.051	0.060	0.056	0.060
7	0.000	0.016	0.016	0.023	0.028	0.037	0.045	0.043	0.049
8	0.000	0.008	0.008	0.013	0.016	0.023	0.030	0.030	0.033
9	0.000	0.005	0.005	0.006	0.011	0.016	0.021	0.020	0.024
10	0.000	0.004	0.003	0.004	0.007	0.010	0.016	0.016	0.019
11	0.000	0.002	0.001	0.003	0.005	0.007	0.009	0.008	0.010
12	0.000	0.001	0.001	0.001	0.003	0.004	0.005	0.005	0.006
13	0.000	0.001	0.001	0.001	0.002	0.003	0.004	0.003	0.004
14	0.000	0.001	0.001	0.001	0.002	0.003	0.004	0.002	0.003

The shower development tables describe the shower from the point of the primary interaction. As described in the text, an interaction was forced in the first counter by requiring the pulse height in the first counter to be larger than a minimum value (see Table A.3). Other conditions were applied to discriminate against background particles. All the conditions are summarized in Table A.3 .

TABLE A.3

Events selection criteria. Conditions are in terms of singly ionizing signals. C1-C14 denote the counter numbers (placed every 4" of steel).

Momentum (GeV)	Conditions
5	- , - , - , C13 < 0.2 , C14 < 0.2
10	C1 > 2.0 , C2 > 0.9 , C3 > 0.3 , C13 < 0.3 , C14 < 0.3
20	C1 > 4.0 , C2 > 0.9 , C3 > 0.9
30	C1 > 5.0 , C2 > 2.0 , C3 > 1.0
50	C1 > 5.0 , C2 > 2.0 , C3 > 1.0
100	C1 >10.0
150	C1 >10.0
200	C1 >10.0
250	C1 >10.0

As can be ascertained from table A2, the average fractional energy deposition in the back half of the calorimeter is small. However, at high energies there are always events where a large fraction of the energy is deposited in the back half. This point is illustrated in figure 8 where the distributions of pulse heights in the first half of the calorimeter are compared to the distributions of pulse heights in the entire calorimeter. The low energy tails are clearly evident. In general, low energy tails are characteristic of lack of containment (figure 8) while high energy tails are characteristic of infrequent sampling (figures 7a and 7b).

Appendix B: Additional Studies and Various Corrections

As described in the main text, there were conditions and corrections applied to the data in order to eliminate possible biases between charged particle induced showers in the test calorimeter and neutrino induced showers in the large area calorimeter. These are summarized below.

1. Background from muons and low energy electrons were removed.
2. An interaction was forced in the first module in order to ensure containment of the shower at high energies. Where applicable, corrections for non-containment were applied.
3. The dependence of the resolution on the steel spacing was investigated in order to understand the dependence of the resolution on the angle with respect to the calorimeter axis of neutrino induced hadron showers.
4. The first interaction of hadrons in the test calorimeter tends to occur in the front part of the first module, while neutrino interactions in the large area calorimeter occur uniformly through the 4" of steel. The low energy data were corrected for this bias.

The first three points were discussed in detail in the main text. The fourth point is discussed in this appendix.

The difference between neutrino interactions which occur uniformly through the 4" of the steel module and hadron interactions which tend to occur near the front part of the module is that in the test calorimeter we tend to sample the shower at a later stage of development. We tested for this bias by replacing the 4" steel modules with 2" steel modules and compared the pulse height distribution of the sum of the 7 even counters (late sampling) with that of the sum of the 7 odd counters (early sampling). The average of the two distributions simulates the case of neutrino interactions where the sampling stage is unknown as the interactions occur uniformly throughout the steel. At 50 GeV, the means

of the average and even distributions were the same. At 10, 20, and 30 GeV, the means of the average distributions were 2.2% higher than those of the even distributions. Therefore, a correction factor of 1.022 was applied to the means of the 10, 20, and 30 GeV distributions of the 4" data. The corresponding correction factor for the 5 GeV data was 1.10. The magnitudes of these corrections are comparable to the errors at these energies. The effect of late sampling is even more noticeable for 8" sampling. The means of the distributions of pulse heights summed over the 7 even counters for the 4" running, (shown in figures 7 a and 7b) are 18.6, 45.3, 71.3, 129, 365, 388, 473, and 574 singly ionizing signals for the energies, 10, 20, 30, 50, 100, 150, 200, and 250 GeV respectively. When compared to the values given by 0.5 times the means of the pulse heights summed over all 14 counters, the means of the even distributions are 29%, 15%, 13%, 4%, 1%, 10%, and 11% lower respectively.

As mentioned earlier, the transverse dimensions of the test calorimeter were 10" by 14". The overall length of the calorimeter was 71". When the 4" steel slabs were replaced by 2" steel slabs the overall length of the calorimeter remained the same, as the scintillator positions were fixed. Because of the drastic reduction in density and the drastic reduction in the amount of steel in the longitudinal direction, the calorimeter in the 2" spacing configuration could not contain high energy showers in the longitudinal direction (see the shower development tables in Appendix A). Even at low energies ($E \leq 50$ GeV), the reduced density resulted in a 23% energy loss out the sides of the calorimeter. This side loss could not affect the results of the above test much because we were only looking for a difference between the even and odd counters. Unlike hadron showers, electron showers are well collimated and of shorter range. Therefore, electron showers were fully contained within the calorimeter in the 2" configuration. The lack of containment of the hadron showers resulted in a clear separation between the electron and hadron peaks. Electron signals were studied by removing the lead absorber that was normally placed upstream of the calorimeter. At 4" spacing (obtained by summing the even counters in the 2" configuration) the distribution for 50 GeV electrons was Gaussian with a mean at 335 singly ionizing signals and rms. width of 7.1%.

A different kind of bias may result if the particle composition of pion induced hadron final states ($\pi^- + p \rightarrow$ hadrons) is different from that of current (W boson) induced hadron final states ($W^- + p \rightarrow$ hadrons). The difference occurs because final state π_o's immediately decay and initiate electromagnetic showers in which the energy loss due to nuclear disintegrations is small, thus electromagnetic showers produce signals which are typically 25% larger than hadron shower

signals. The resulting bias is probably small because it changes the calibration by only 25% of the fractional difference between the π_o composition of pion induced hadronic final states and that of current induced hadronic final states. Eventually even this small bias may be removed when more information is available about the particle composition of current induced hadron final states. It may also be possible to eliminate the bias by using the information in the longitudinal development of the shower to estimate the initial π_o composition in the hadron final state for each event.

Appendix C: Fitting Poisson Distributions

As mentioned in the main text, the pulse height distributions of hadrons in the calorimeter were best represented by Poisson distributions. The Poisson distribution is an integral distribution; we transform it into a continuous distribution in the following manner. The integral Poisson distribution for N events is:

$$P(n) = N\, e^{-\bar{n}}\, \frac{(\bar{n})^n}{n!}$$

where $\bar{n}$ is the mean of the distribution. We make the following transformation: $n \to x/a$, $\bar{n} \to \bar{x}/a$, $n! \to \Gamma\,(x/a + 1)$.

$$y(x) = \frac{b\, e^{-(\bar{x}/a)} \left(\frac{\bar{x}}{a}\right)^{(x/a)}}{\Gamma\,(x/a + 1)}$$

Here y is the number of events per bin and x is in units of equivalent particle signals. We have used the following approximation for the Γ function:

$$\Gamma\,(z) = z^z\, e^{-z}\, \frac{\sqrt{2\pi z}}{z} \left[1 + \frac{1}{12z} + \frac{1}{288z^2}\right]$$

We obtained the best values for a, b and $\bar{x}$ by minimizing the chi-squared of the fit using a non-linear fitting routine. The best fit mean of the distribution is $\bar{x}$, the resolution $(\sigma/\bar{x}) = \sqrt{(a/\bar{x})}$, and the area under the fit is b/a.

References

1. B. C. Barish, J. F. Bartlett, K. W. Brown, D. Buchholz, F. Jacquet, F. S. Merritt, F. J. Sciulli, H. Suter, H. E. Fisk, and G. Krafczyk, Phys. Rev. Lett. 34, 538 (1975); ibid 32, 1387 (1974); ibid 31, 180, 410, 565 (1973).

2. V. S. Murzin, in Progress in Elementary Particles and Cosmic Ray Physics, Vol. 9, page 245 (eds. J. G. Wilson and S. A. Wouthuysen; North-Holland Publ. Co., Amsterdam, 1967).

3. J. Engler, W. Flauger, B. Gibbard, F. Monning, K. Runge and H. Schopper, Nucl. Instr. and Meth. 106 (1973) 189; H. Whiteside, C. J. Crannell, H. Crannell, J. F. Ormes, M. J. Ryan and W. V. Jones, Nucl. Instr. and Meth. 109 (1973) 375.

4. B. C. Barish, J. F. Bartlett, D. Buchholz, T. Humphrey, F. S. Merritt, Y. Nagashima, F. J. Sciulli, D. Shields, H. Suter, G. Krafczyk and A. Maschke, Nucl. Instr. and Meth. 116 (1974) 413.

5. R. M. Sternheimer and R. F. Peierls, Brookhaven National Laboratory preprint BNL 15518 (Jan. 1971).

6. J. Lach and S. Pruss, Fermilab Technical Memo, TM-285, 2254.00 (Jan.1971).

7. If there is some energy loss out the sides of the test calorimeter, and the beam is aimed at points away from the center of the calorimeter, the energy loss on one side may be partially compensated by an energy gain on the other side, thus resulting in only a small change in the signal.

8. F. J. Sciulli, Rapporteur talk on Photon-Collecting Hadron Calorimeters, proceedings of the Calorimeter Workshop, Fermilab, May 1975 (also available as CALT 68-502 preprint); the Monte-Carlo calculations are based on the work of W. V. Jones, Phys. Rev. 187, 1868 (1969).

9. We have used the following fit to the mean DE/DX energy loss of muons in steel: DE/DX (MeV/cm) = $12.45\,P^{0.06544}$, where the momentum P is in GeV ($P > 1$ GeV).

10. The negative sign selected beam is primarily composed of pions. For pions in our energy range the momentum P = E, and is a good approximation to the kinetic energy T, since T = E - 0.14.

11. Note that a possible 3% to 6% energy loss out the sides of the calorimeter at low energies may also cause a departure from linearity.

Figure 1 - Schematic of the test calorimeter.

Figure 2 - Pulse height distribution of singly ionizing particles in the first counter. (a) 150 GeV hadrons, steel plates removed. (b) 50 GeV muons, 4" steel plates in place.

Figure 3 - Pulse height distribution summed over 14 counters for 50 GeV muons, (4" steel plates in place).

Figure 4a - Pulse height distributions summed over 14 counters for 5, 10, 20, 30, and 50 GeV hadrons, (4" steel spacing).

Figure 4b - Pulse height distributions summed over 14 counters for 100, 150, 200, and 250 GeV hadrons, (4" steel spacing). The curves are the best fit poisson distributions.

Figure 5a - The mean number of equivalent singly ionizing particles deposited in the calorimeter vs. the incident hadron energy, (4" steel spacing). The curve corresponds to the fit described in the text.

Figure 5b - The rms resolution of the calorimeter vs. the incident hadron energy, (4" steel spacing). The curve corresponds to $1.105/\sqrt{E}$.

Figure 6 - The resolution at 200 GeV vs. spacing between counters.

Figure 7a - Pulse height distributions (8" spacing) for 10, 20, 30, and 50 GeV hadrons. The curves are the best fit poisson distributions.

Figure 7b - Pulse height distributions (8" spacing) for 100, 150, 200, and 250 GeV. The curves are the best fit poisson distributions.

Figure 8 - Non-containment effects illustrated by the pulse height distributions in the first half of the calorimeter.

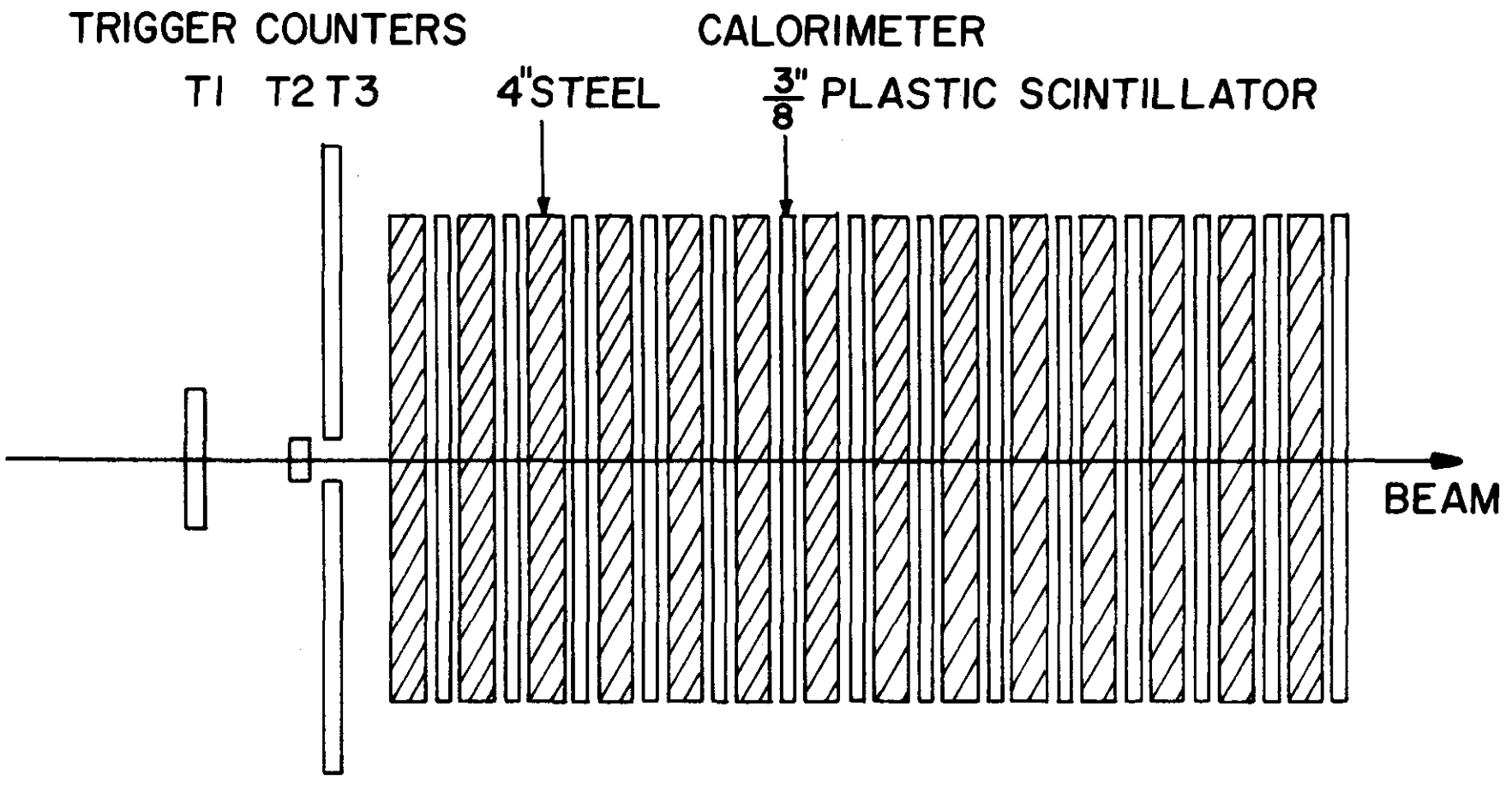
TRIGGER COUNTERS
T1 T2 T3
CALORIMETER
4"STEEL
3/8" PLASTIC SCINTILLATOR
BEAM

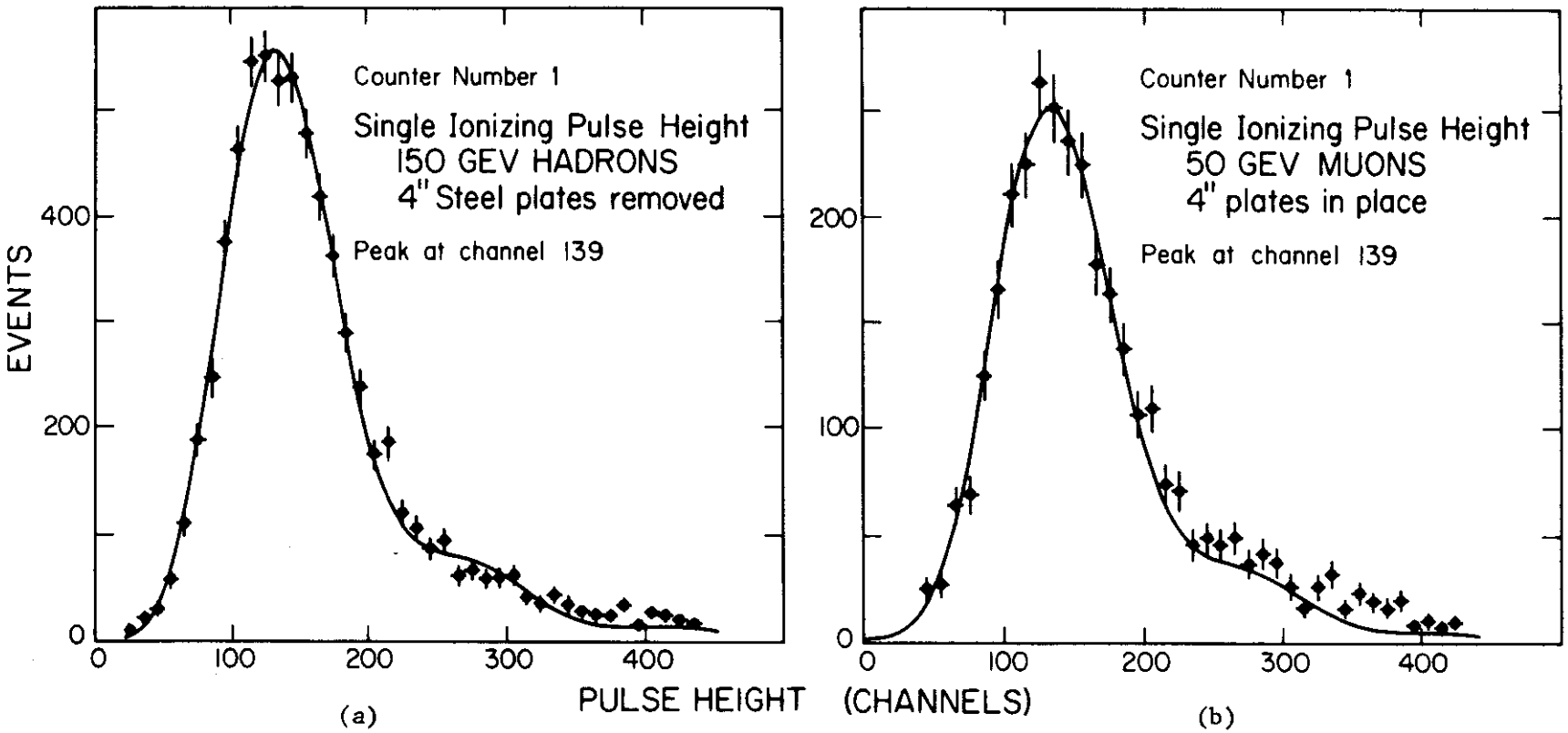
Counter Number 1
Single Ionizing Pulse Height
150 GEV HADRONS
4" Steel plates removed
Peak at channel 139
EVENTS
0
200
400
0
100
200
300
400
PULSE HEIGHT (CHANNELS)
(a)
Counter Number 1
Single Ionizing Pulse Height
50 GEV MUONS
4" plates in place
Peak at channel 139
0
100
200
0
100
200
300
400
(b)

Fig. 2

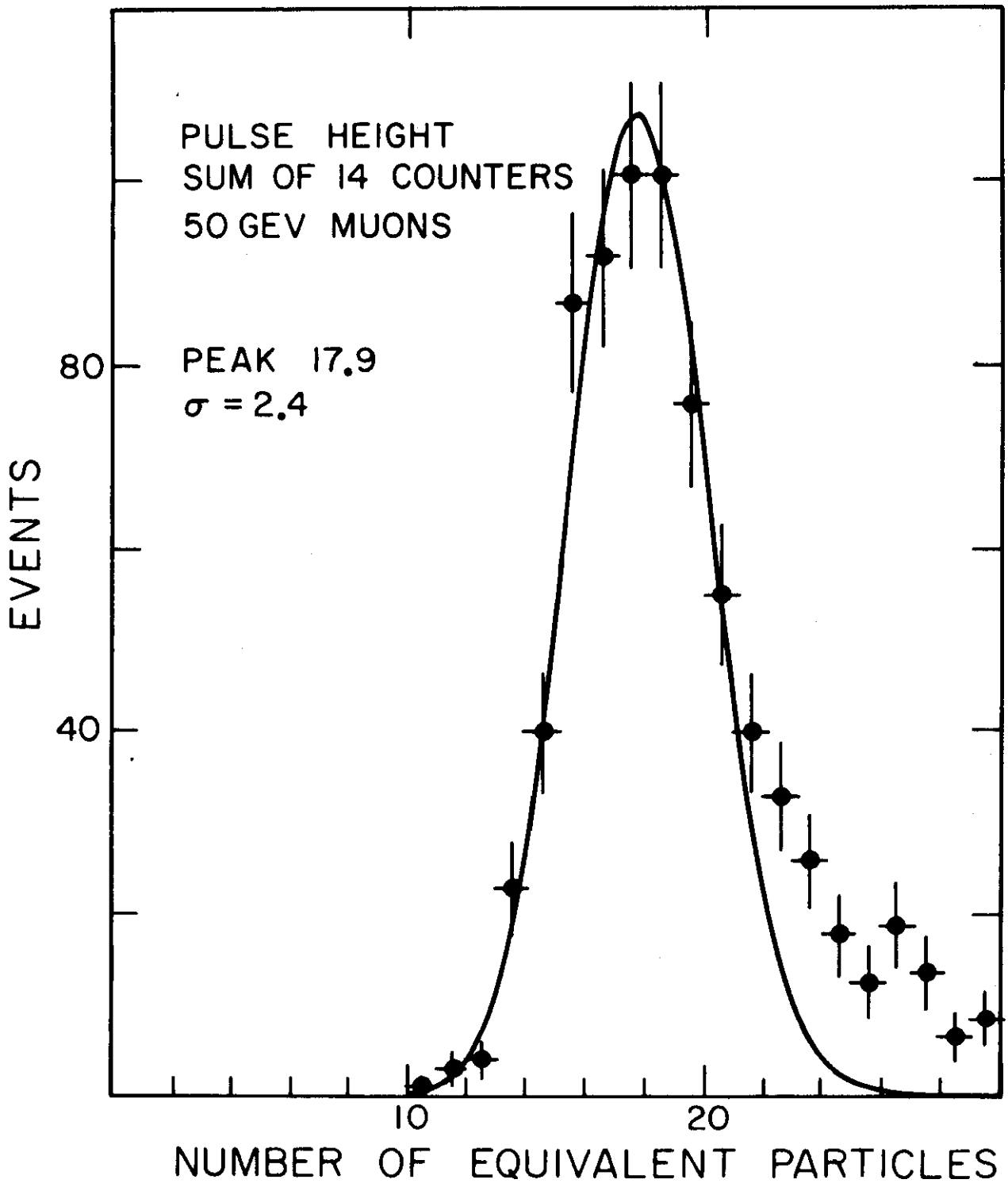
PULSE HEIGHT
SUM OF 14 COUNTERS
50 GEV MUONS
PEAK 17.9
σ = 2.4
80
40
EVENTS
10
20
NUMBER OF EQUIVALENT PARTICLES

Fig. 3

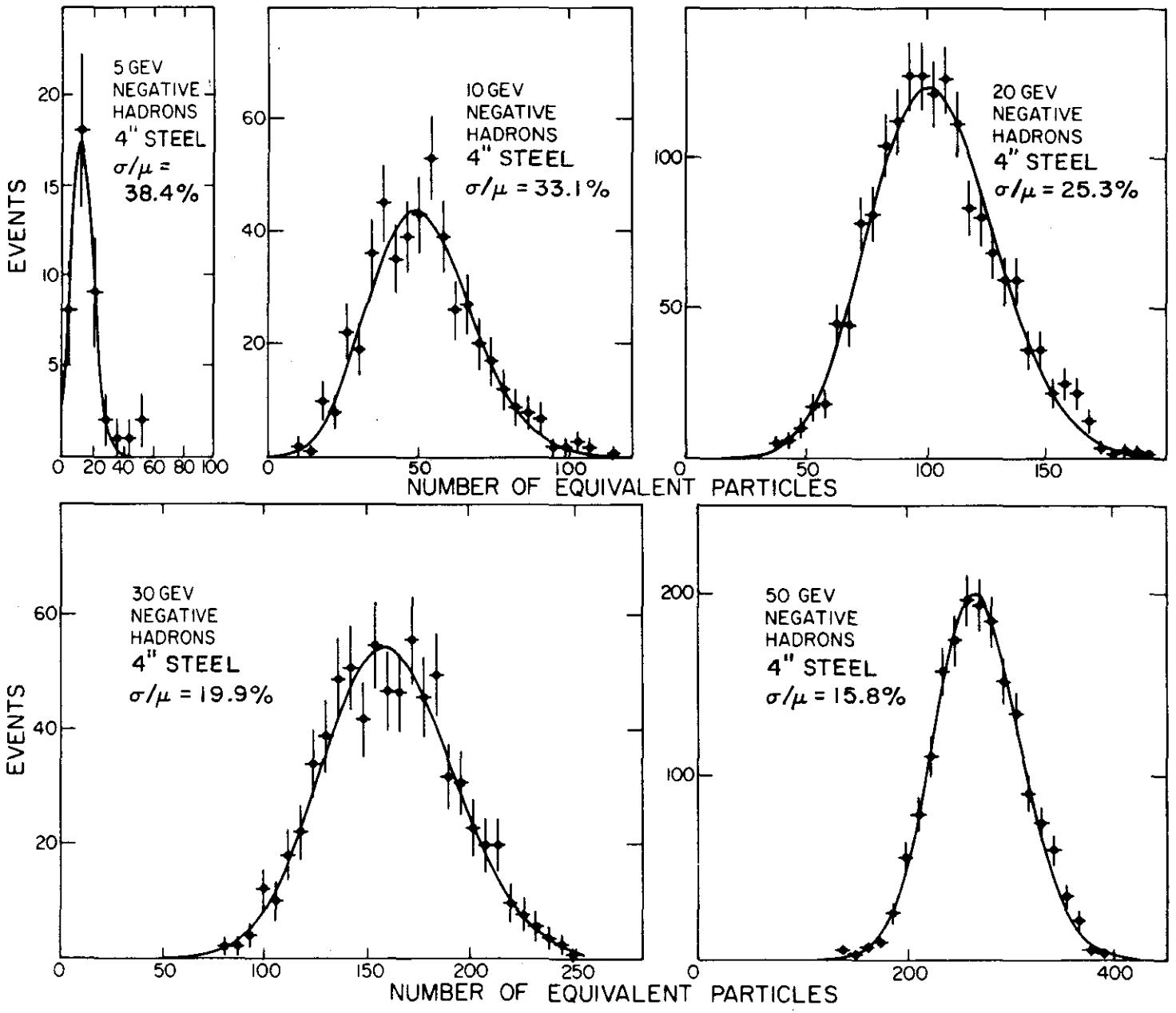
5 GEV
NEGATIVE
HADRONS
4" STEEL
σ/μ =
38.4%
10 GEV
NEGATIVE
HADRONS
4" STEEL
σ/μ = 33.1%
20 GEV
NEGATIVE
HADRONS
4" STEEL
σ/μ = 25.3%
30 GEV
NEGATIVE
HADRONS
4" STEEL
σ/μ = 19.9%
50 GEV
NEGATIVE
HADRONS
4" STEEL
σ/μ = 15.8%
EVENTS
NUMBER OF EQUIVALENT PARTICLES

Fig. 4a

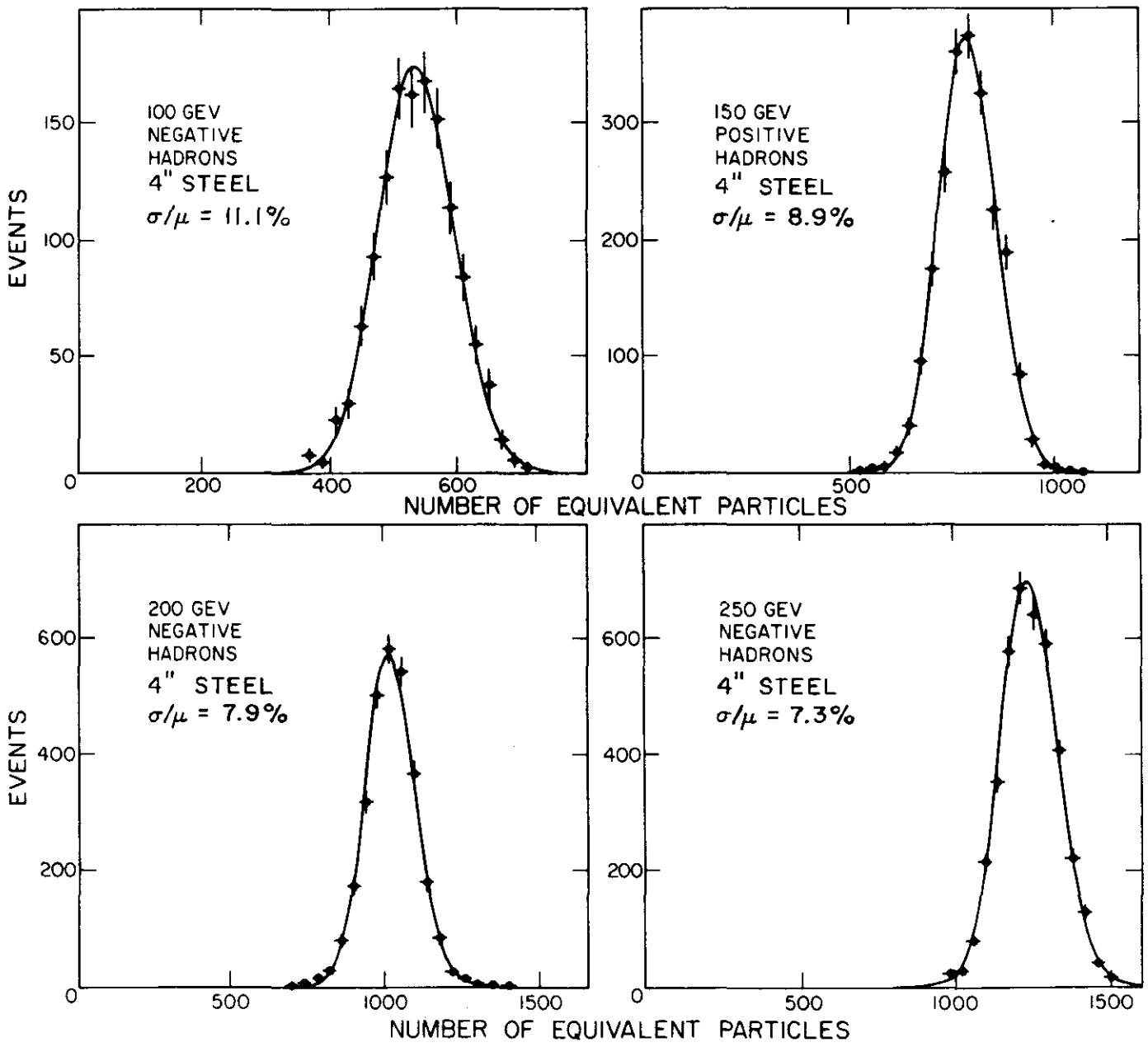
100 GEV
NEGATIVE
HADRONS
4" STEEL
σ/μ = 11.1%
150 GEV
POSITIVE
HADRONS
4" STEEL
σ/μ = 8.9%
200 GEV
NEGATIVE
HADRONS
4" STEEL
σ/μ = 7.9%
250 GEV
NEGATIVE
HADRONS
4" STEEL
σ/μ = 7.3%
EVENTS
NUMBER OF EQUIVALENT PARTICLES

Fig. 4b

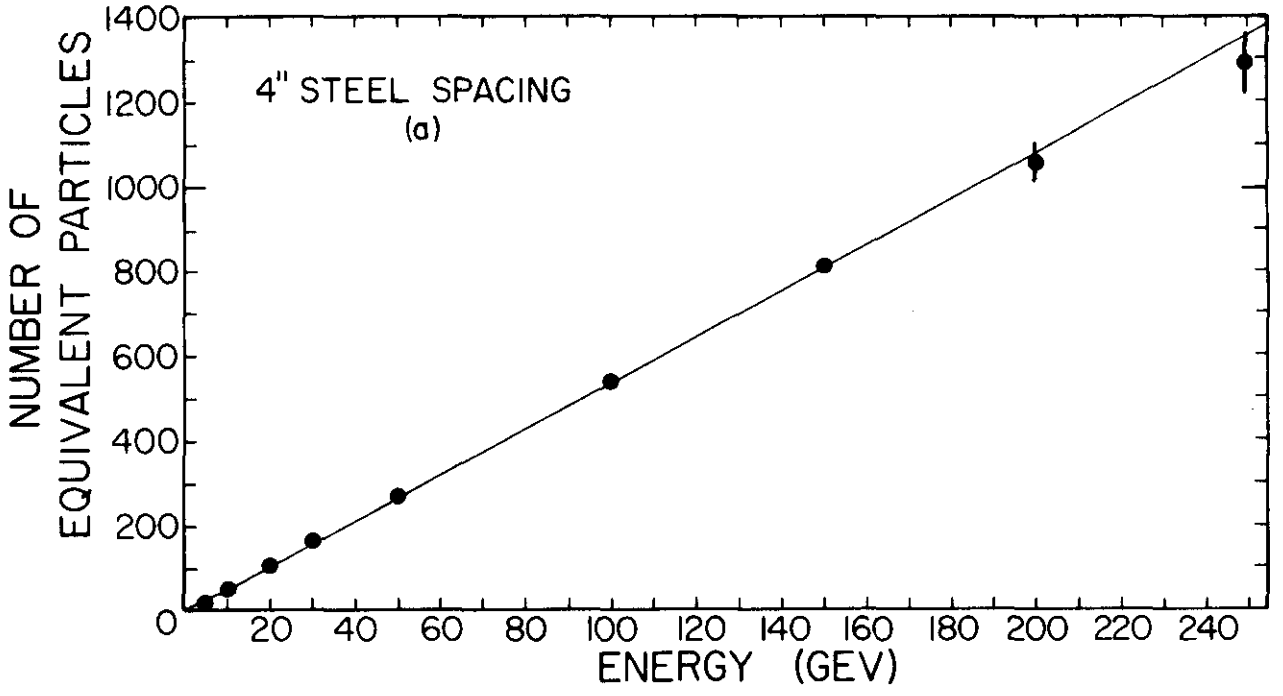
4" STEEL SPACING
(a)
NUMBER OF
EQUIVALENT PARTICLES
1400
1200
1000
800
600
400
200
0
20
40
60
80
100
120
140
160
180
200
220
240
ENERGY (GEV)

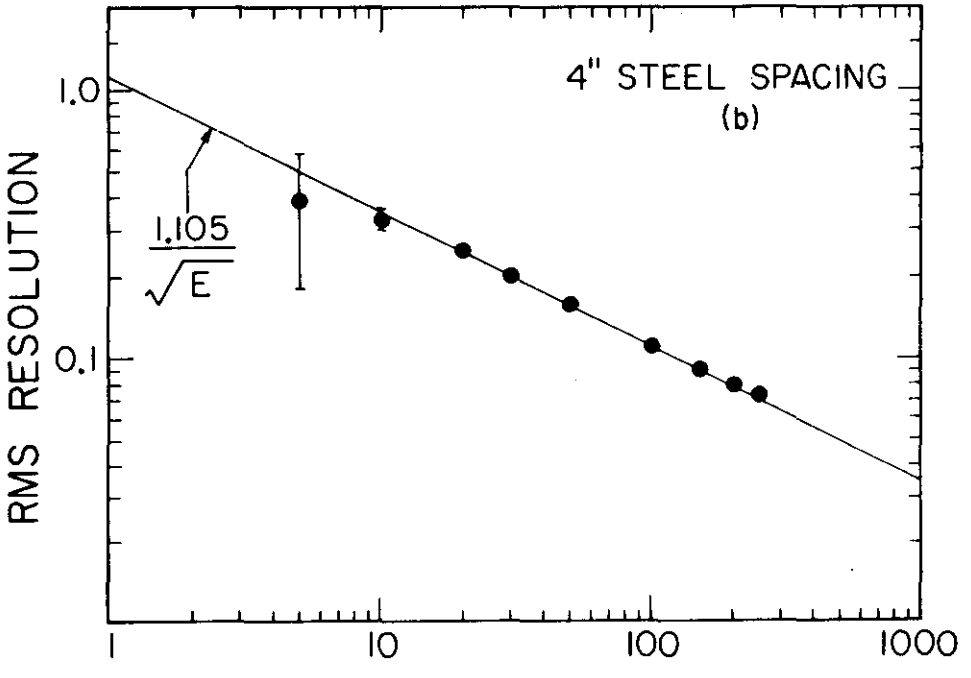
4" STEEL SPACING
(b)
RMS RESOLUTION
1.0
0.1
1.105
√E
1
10
100
1000

Fig. 5

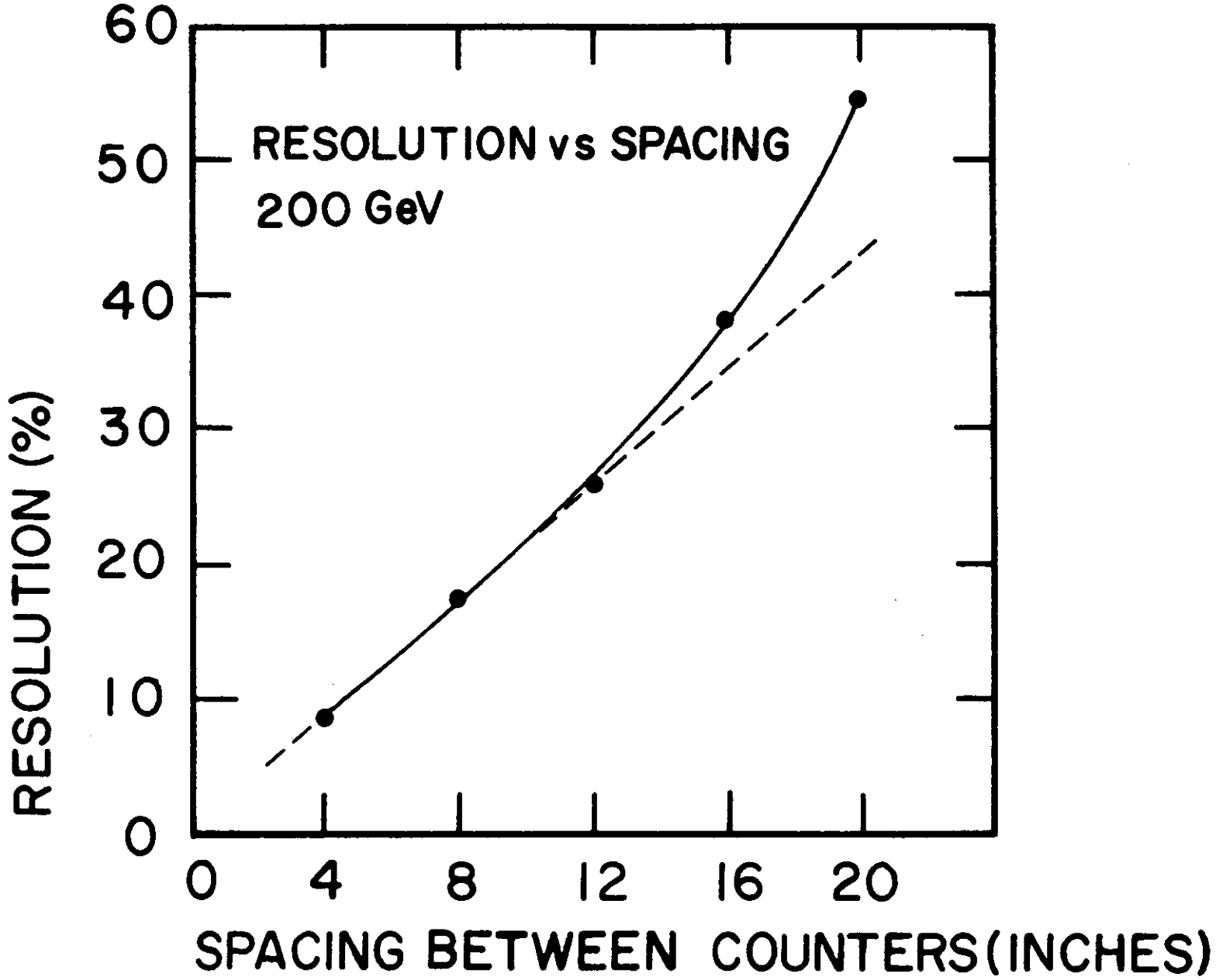
RESOLUTION vs SPACING
200 GeV
RESOLUTION (%)
0
10
20
30
40
50
60
0
4
8
12
16
20
SPACING BETWEEN COUNTERS (INCHES)

Fig. 6

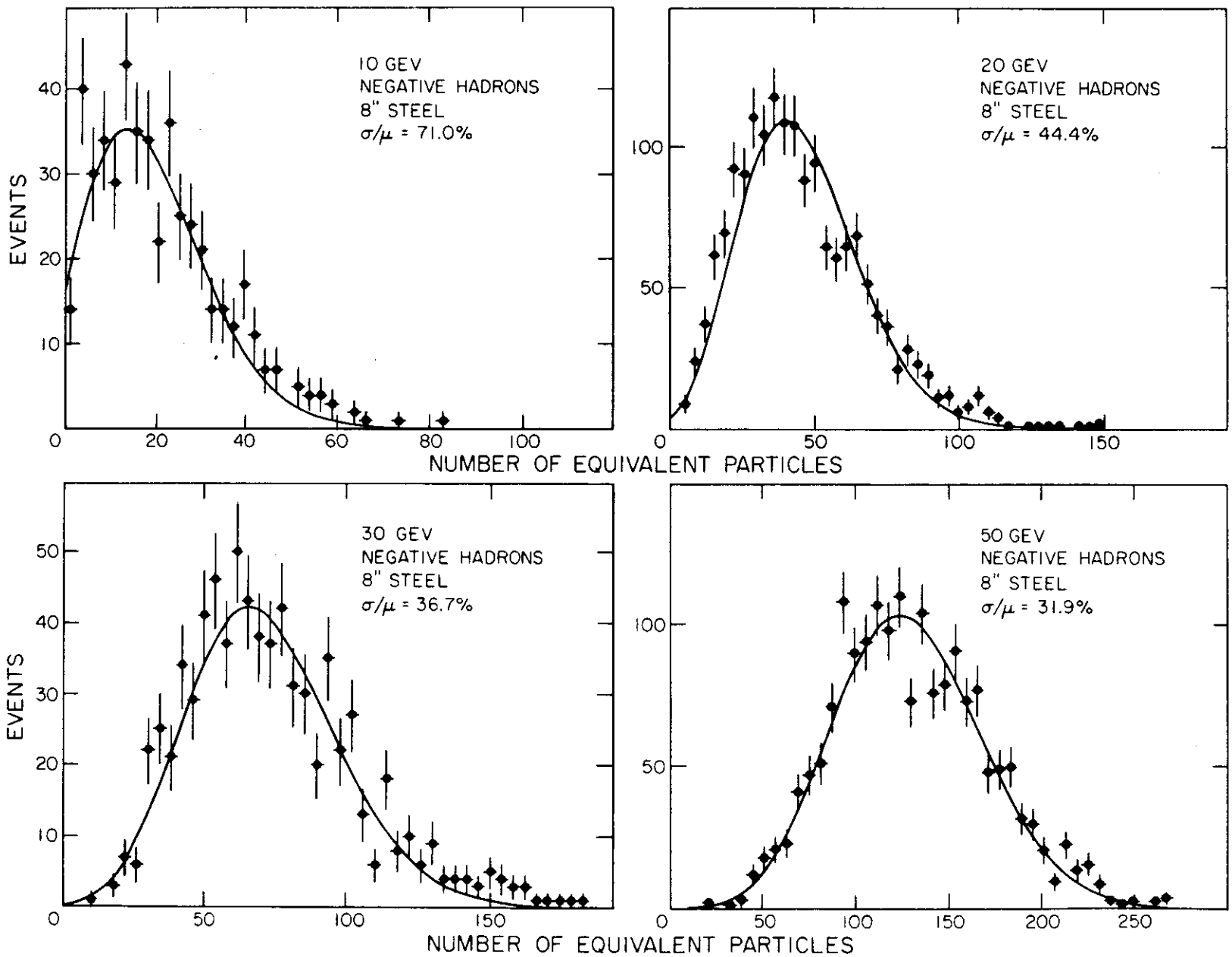
10 GEV
NEGATIVE HADRONS
8" STEEL
σ/μ = 71.0%
20 GEV
NEGATIVE HADRONS
8" STEEL
σ/μ = 44.4%
30 GEV
NEGATIVE HADRONS
8" STEEL
σ/μ = 36.7%
50 GEV
NEGATIVE HADRONS
8" STEEL
σ/μ = 31.9%
EVENTS
NUMBER OF EQUIVALENT PARTICLES

Fig. 7a

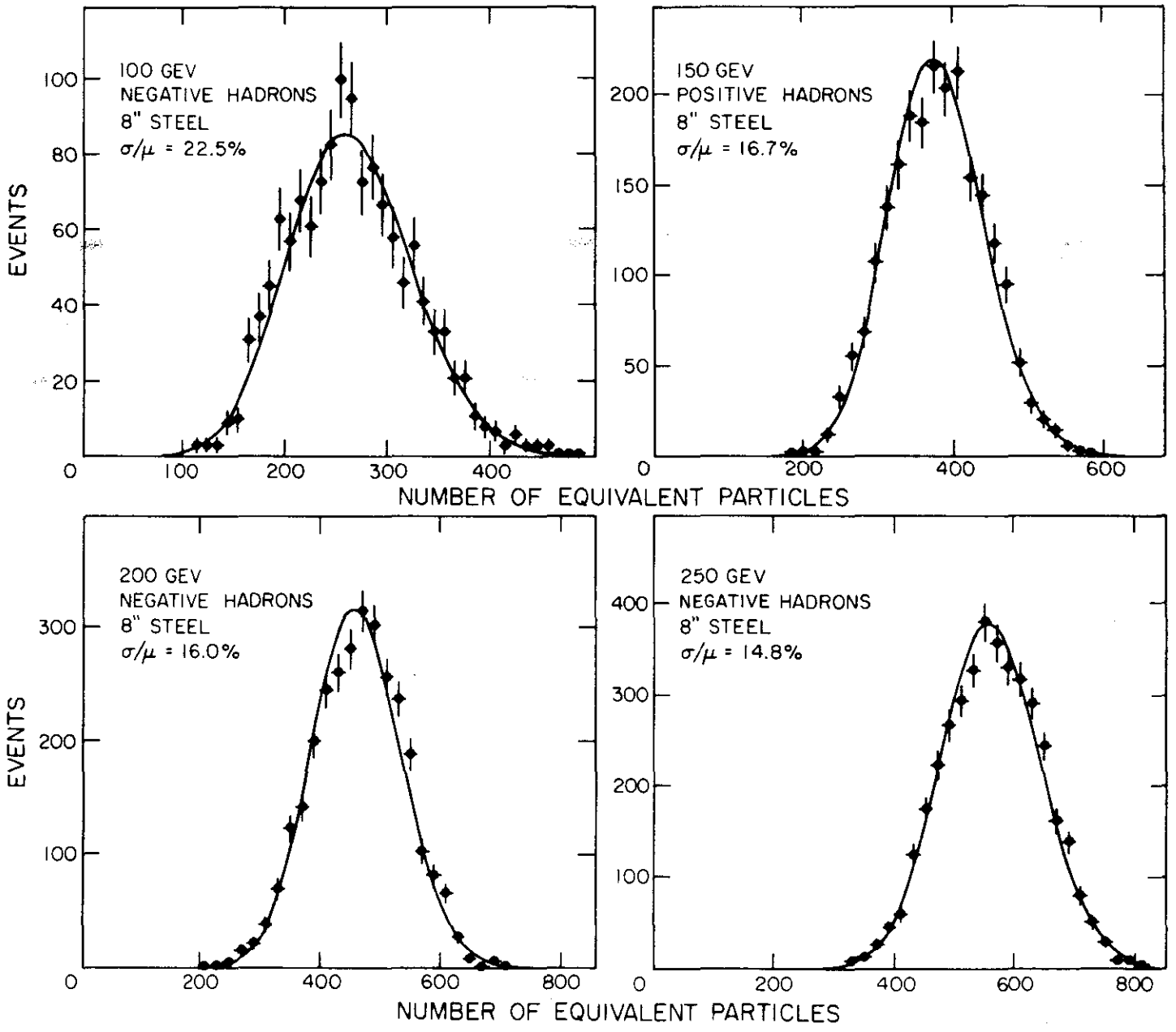
100 GEV
NEGATIVE HADRONS
8" STEEL
σ/μ = 22.5%
150 GEV
POSITIVE HADRONS
8" STEEL
σ/μ = 16.7%
200 GEV
NEGATIVE HADRONS
8" STEEL
σ/μ = 16.0%
250 GEV
NEGATIVE HADRONS
8" STEEL
σ/μ = 14.8%
EVENTS
NUMBER OF EQUIVALENT PARTICLES

Fig. 7b

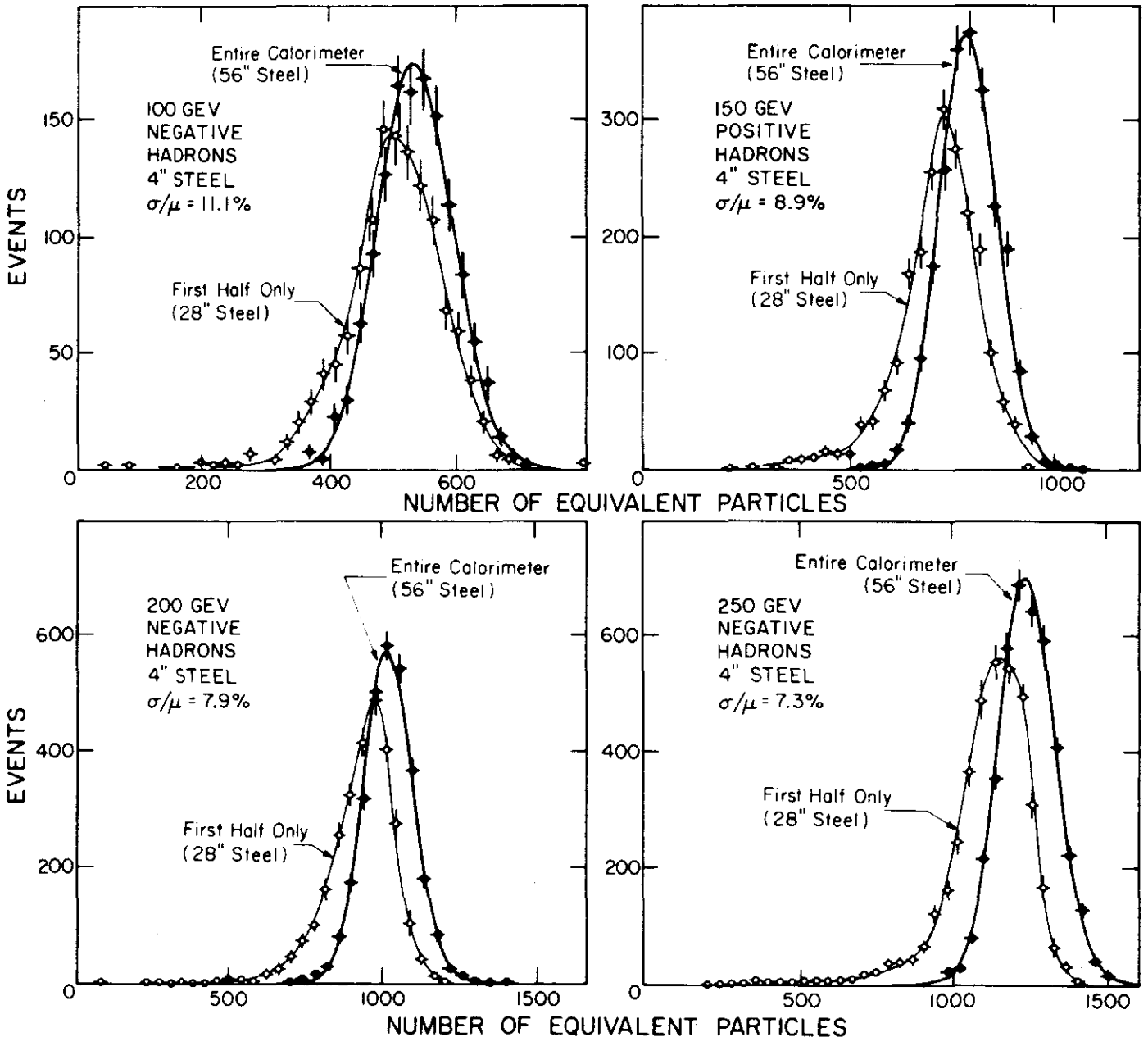
Entire Calorimeter
(56" Steel)
100 GEV
NEGATIVE
HADRONS
4" STEEL
σ/μ = 11.1%
First Half Only
(28" Steel)
EVENTS
150
100
50
0
200
400
600
Entire Calorimeter
(56" Steel)
150 GEV
POSITIVE
HADRONS
4" STEEL
σ/μ = 8.9%
First Half Only
(28" Steel)
300
200
100
0
500
1000
NUMBER OF EQUIVALENT PARTICLES
Entire Calorimeter
(56" Steel)
200 GEV
NEGATIVE
HADRONS
4" STEEL
σ/μ = 7.9%
First Half Only
(28" Steel)
EVENTS
600
400
200
0
500
1000
1500
Entire Calorimeter
(56" Steel)
250 GEV
NEGATIVE
HADRONS
4" STEEL
σ/μ = 7.3%
First Half Only
(28" Steel)
600
400
200
0
500
1000
1500
NUMBER OF EQUIVALENT PARTICLES

Fig. 8